



## Study of different triazole derivative inhibitors to protect copper against pitting corrosion

W. QAFSAOUI<sup>1,2</sup>, Ch. BLANC<sup>1</sup>, N. PÉBÈRE<sup>1</sup>, A. SRHIRI<sup>3</sup> and G. MANKOWSKI<sup>1</sup>

<sup>1</sup>Laboratoire Interfaces et Matériaux, UPRESA CNRS 5071 ENSCT, 118, route de Narbonne, 31077 Toulouse Cedex 04, France

<sup>2</sup>Faculté des Sciences d'El Jadida, Morocco

<sup>3</sup>Laboratoire d'Electrochimie, Faculté des Sciences de Kénitra, Morocco

Received 17 August 1999; accepted in revised form 4 January 2000

**Key words:** copper, EIS, inhibition, pitting, XPS

### Abstract

Electrochemical experiments were performed to study the inhibitive effect towards copper corrosion of three organic compounds: namely, benzotriazole, 1-hydroxybenzotriazole and 3-amino 1,2,4-triazole. Statistical analysis of pit nucleation times showed that 3-amino 1,2,4-triazole exhibited the most significant inhibitive effect towards pitting. However, impedance measurements revealed that this compound produced a thinning of the passive film. This was corroborated by X-ray photoelectron spectroscopy. Results showed that copper pitting resistance could not be explained only by characterizing the protectiveness of the passive film.

### 1. Introduction

Copper presents good resistance to corrosion in natural water and is widely used in water distribution networks. However, in some environments containing species such as chloride, sulphate or nitrate [1–3] passive film breakdown may occur leading to the propagation of pits. Pit nucleation occurs when the potential is higher than a critical potential and, generally, after a period termed the pit nucleation time. Often, nucleation times are widely scattered. Thus, experimental data must be statistically analysed. Such analysis allows the pit nucleation rate to be determined [4, 5].

For fifty years, benzotriazole (BTAH) has been well-known for its inhibitory action on copper and copper alloy dissolution. Numerous studies [6–21] have been devoted to the evaluation of its effectiveness in different media and to the elucidation of its action mechanisms. Some points are now well established. The benzotriazole molecule acts through a  $[\text{Cu}^+-\text{BTA}^-]_n$  complex involving Cu–N bonds leading to the formation of an insoluble polymeric film [11–13]. The oxide film, especially the  $\text{Cu}_2\text{O}$  layer, seems to be important in the mechanism of the polymeric film formation [18–20] but some authors have claimed that this film can be built up on a clean copper surface [16, 17].

Other authors [22] have studied the inhibitive effect of 'triazole'-type compounds (i.e., triazole, bitriazole and aminotriazole) on a cupronickel alloy in chloride solutions. They showed that aminotriazole is the most

efficient inhibitor, acting by modification of the kinetic control of the cathodic reaction.

Although the efficiency of benzotriazole and other derivatives from triazole towards copper dissolution has been extensively investigated, the influence of these inhibitors on the susceptibility to localized corrosion has not been specifically studied. In this work, we investigated the influence of benzotriazole (BTAH), 1-hydroxybenzotriazole (BTAOH) and 3-amino 1,2,4-triazole (ATA) on the pit nucleation susceptibility of pure copper in chloride-containing borate-buffered solutions. In addition, current–voltage curves and electrochemical impedance measurements were performed to study the behaviour of the copper–solution interface in the presence of the different inhibitors.

### 2. Experimental methods

#### 2.1. Materials

The material used in this investigation was pure copper (99.99%) supplied in the form of a drawn copper rod. Ten specimens of the material were machined into 8 mm diameter and 10 mm length cylinders and embedded in epoxy resin on the same holder. They were tested simultaneously using a data acquisition system which allowed the current versus time to be recorded for each specimen.

BTAH ( $C_6H_5N_3$ ) was supplied by Prolabo and BTAOH ( $C_6H_5N_3O$ ) and ATA ( $C_2H_4N_4$ ) by Sigma. The purities of these compounds were 98%, 88% and 95%, respectively.

### 2.2. Statistical analysis of pitting

Before testing, the specimens were mechanically polished to 1000 grit SiC paper and rinsed with distilled water. They were then potentiostatically polarized for a time  $t_p$  in a borate-buffered solution ( $0.01 \text{ M H}_3\text{BO}_3 + 0.01 \text{ M Na}_2\text{B}_4\text{O}_7$ ) (pH 9) with or without the presence of BTAH, BTAOH or ATA. This time ( $t_p$ ) of prepolarization allowed an oxide film to grow on the specimen surface. Then, a chloride-containing buffered solution was injected into the medium in such a way that the final concentration of chloride was  $0.2 \text{ M}$ . All the experiments were performed at room temperature ( $22 \text{ }^\circ\text{C}$ ). The first pit appeared on each specimen after randomly dispersed nucleation times which corresponded to a sudden increase in the anodic current. The distributions of nucleation times were determined from 100 measurements resulting from 10 experiments. The distribution curve was obtained by plotting  $-\ln[1 - P(t)]$  against  $t$ , where  $P(t)$  is the pitting probability calculated from the experimental data such as  $n(t)/N$  ( $n(t)$  being the number of specimens in which pitting occurred at time  $t$  and  $N$  the total number of specimens). The slope  $\lambda_0$  of the distribution curve at its origin is the pit nucleation rate and is representative of the resistance of the film developed at the end of the prepolarization period. So, the value of  $\lambda_0$  was used to assess and compare the pitting susceptibility of copper under different experimental conditions [5].

### 2.3. Impedance measurements

For electrochemical impedance measurements, the working electrode was a rotating disk consisting of a copper rod of  $0.2 \text{ cm}^2$  cross-sectional area. A thermoretractable sheath preventing the cylindrical area from making contact with the solution, the electrode surface was only the cross-section. All the experiments were performed with a rotation rate of 1000 rpm. Electrochemical impedance measurements were carried out using a Solartron 1250 frequency response analyser (8 points by decade) with a Solartron 1286 electrochemical interface.

### 2.4. Potentiokinetic curves and XPS analyses

The experiments were completed by plotting of potentiokinetic curves in borate-buffered solutions containing  $0.2 \text{ M}$  chloride and  $10^{-4} \text{ M}$  or  $10^{-2} \text{ M}$  of BTAH, BTAOH or ATA. The scanning potential rate was  $1200 \text{ mV h}^{-1}$ . The XPS measurements were carried out on a VG Escalab MKII. The specimens were irradiated with a  $\text{AlK}_\alpha$  X-ray source.

## 3. Results and discussion

### 3.1. Evaluation of inhibitor efficiency on the pit nucleation rate

Statistical analysis was performed to evaluate the pit nucleation rate on copper samples polarized in borate buffered solutions containing one of the three inhibitors tested, namely, BTAH, BTAOH and ATA. Figure 1 shows the logarithm of the pit nucleation rate  $\lambda_0$  versus inhibitor concentration for the three inhibitors. The dotted line represents the pit nucleation rate measured in inhibitor-free solution.

BTAH and BTAOH show similar behaviour since the same critical concentration for inhibitory effect can be determined for these two inhibitors. For inhibitor concentrations in the range  $1 \times 10^{-6}$  to  $5 \times 10^{-4} \text{ M}$ , the two compounds exhibit no inhibitory effect. For inhibitor concentrations higher than  $5 \times 10^{-4} \text{ M}$ , the pit nucleation rate rapidly decreases as the inhibitor (BTAH or BTAOH) concentration increases, showing nearly the same inhibitory effect for the two compounds. For BTAH and BTAOH,  $\log \lambda_0$  varied linearly versus the log of inhibitor concentration in the  $5 \times 10^{-4}$  to  $1 \times 10^{-2} \text{ M}$  range.

For ATA, the same kind of variation of  $\lambda_0$  was also observed, but the critical concentration measured for this inhibitor appears to be lower than that found for the others since it was close to  $2 \times 10^{-6} \text{ M}$ . ATA is thus an efficient inhibitor when at a concentration higher than  $10^{-6} \text{ M}$ . For concentrations between  $2 \times 10^{-6} \text{ M}$  and  $2 \times 10^{-2} \text{ M}$ , ATA seems to be a better inhibitor of copper pitting than BTAH and BTAOH. At  $2 \times 10^{-2} \text{ M}$ , the three compounds have the same efficiency.

### 3.2. Study of ATA inhibitory efficiency

To analyse the inhibitory effect of ATA towards copper pitting, the influence of the polarization potential and that of the polarization duration were studied.

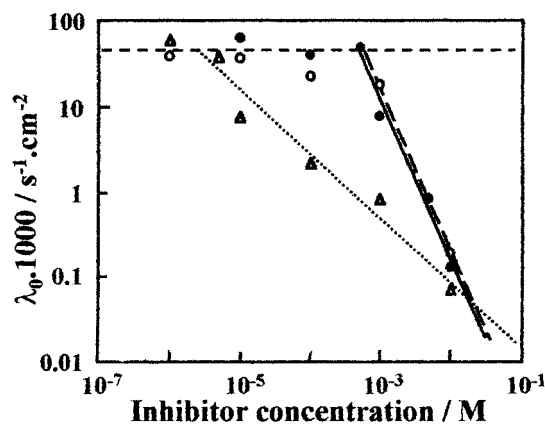


Fig. 1. Pit nucleation rate  $\lambda_0$  against BTAH, BTAOH and ATA concentrations. Copper polarized for 1 h at  $+400 \text{ mV}$  vs SCE in a borate-buffered solution containing one inhibitor. After 1 h,  $0.2 \text{ M}$  chlorides are added. Dotted line indicates the pit nucleation rate measured without inhibitor. Key: (○—○) BTAH, (●—●) BTAOH and (▲—▲) ATA.

Figure 2 shows  $\lambda_0$  against polarization potential for copper polarized in borate-buffered solutions with and without ATA. In both solutions,  $\lambda_0$  increases with applied potential. This shows the activation of copper pitting with potential. However, whatever the applied potential, the  $\lambda_0$  values measured for ATA-containing solutions were lower than those measured in solutions without ATA which confirmed the inhibitory efficiency of the compound. Moreover, Figure 2 shows that a critical potential for pitting can be defined in both solutions without ATA and with ATA. This critical pitting potential corresponds to the potential for which pitting begins to appear. This critical pitting potential shifted from the 100 to 200 mV vs SCE potential range to the 200 to 300 mV vs SCE potential range when ATA was added to the borate-buffered solution. This again shows that ATA has a significant inhibitory effect towards copper pitting.

Figure 3 shows  $\lambda_0$  against polarization duration for copper polarized at +400 mV/SCE in a buffered solution containing  $10^{-4}$  M ATA. The pit nucleation rate decreases when the duration of prepolarization increases. This can be easily explained by a thickening of the passive film as prepolarization continues. Moreover, it can be assumed from the previous results that ATA reacts with the passive film. This variation of  $\lambda_0$  can thus be related to an evolution of the passive film formed in the presence of ATA. Moreover, the pit nucleation rate obeys the following law:

$$\lambda_0 = \lambda_\infty + k/t \quad (1)$$

where  $\lambda_\infty$  represents the maximum resistance obtained by an infinitely long prepolarization. It should be noted that the value of  $\lambda_\infty$  can be assumed to be zero. This shows that film formed in the presence of ATA evolves with time and can become very protective against pitting corrosion. Moreover, a previous study [5] had already shown that  $\lambda_0$  decreased when the prepolarization duration increased when copper was polarized in bo-

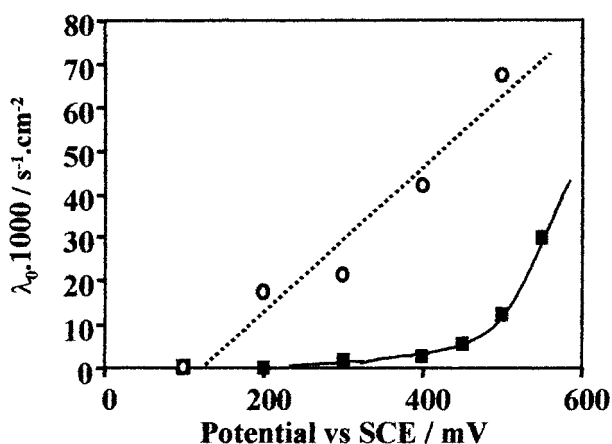


Fig. 2. Pit nucleation rate  $\lambda_0$  against polarization potential. Copper polarized for 1 h in borate-buffered solution with or without  $10^{-4}$  M ATA. After 1 h, 0.2 M chlorides are added. Key: (○) without inhibitor and (■) with ATA.

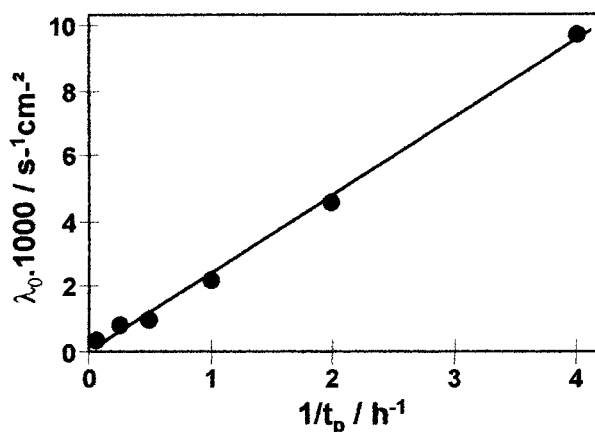


Fig. 3. Pit nucleation rate  $\lambda_0$  against prepolarization time  $t_p$ . Copper polarized at +400 mV vs SCE for a time  $t_p$  in borate-buffered solutions containing  $10^{-4}$  M ATA. Then, 0.2 M chlorides are added.

rate-buffered solutions without inhibitor. In this case, the value of  $\lambda_\infty$ , calculated by extrapolating the straight line observed, was not zero. Therefore, a value of  $\lambda_\infty$  of zero cannot be explained only by thickening of the passive film with time. ATA obviously interacts with this passive film and confers very efficient protection.

Over a large concentration domain, ATA can be considered as the most effective inhibitor for copper pitting. Potentiokinetic polarization curves were then plotted for copper polarized in borate-buffered solutions containing the different inhibitors to compare the results obtained for the statistical analysis for pitting corrosion to the behaviour of copper for generalized corrosion.

### 3.3. Efficiency of BTAH, BTAOH and ATA as inhibitors for generalized corrosion in copper

Potentiokinetic polarization curves were plotted for copper in borate-buffered solutions containing 0.2 M chloride and  $10^{-4}$  M or  $10^{-2}$  M of each inhibitor (Figure 4). The concentrations were chosen to compare the efficiency of the three inhibitors against generalized corrosion of copper when present in solution at a concentration for which ATA was the most effective inhibitor of pitting corrosion ( $10^{-4}$  M) and at a concentration for which the three inhibitors showed a similar efficiency ( $10^{-2}$  M).

Comparison of the curves plotted for copper in solution without inhibitive species and with  $10^{-4}$  M inhibitors shows that BTAH and BTAOH did not induce a significant shift in the pitting potential. In contrast, ATA shifted the pitting potential from 300 to 600 mV vs SCE. This confirms the results obtained by statistical analysis. At low concentrations ATA was the most effective inhibitor of pitting corrosion of copper. At  $10^{-2}$  M, BTAH and BTAOH were efficient against copper pitting since they shifted the pitting potential to 600 mV. For ATA, the passivity plateau was not well defined and the sudden increase in current corresponding to pitting was not easily observed. However, the current became significant at 600 mV vs SCE. There-

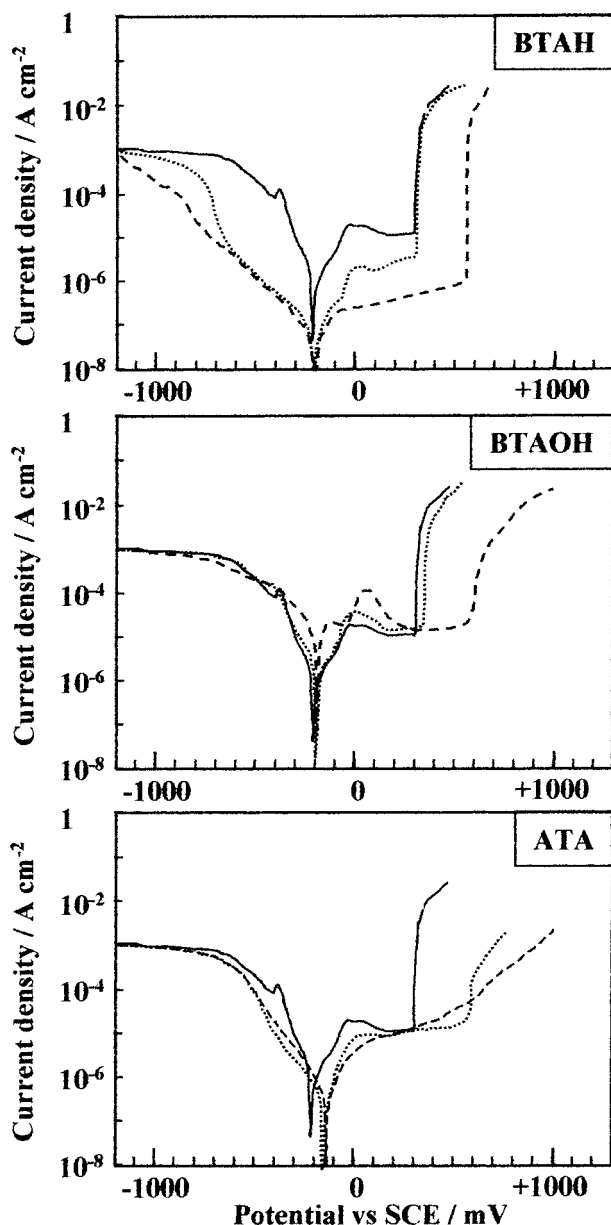


Fig. 4. Potentiokinetic polarization curves plotted on copper in 0.2 M chloride-containing borate-buffered solutions without and in presence of  $10^{-2}$  or  $10^{-4}$  M BTAH, BTAOH or ATA. Key: (—) 0 M, (.....)  $10^{-4}$  M and (— · —)  $10^{-2}$  M.

fore, when the concentration was  $10^{-2}$  M, the three inhibitors showed a similar efficiency with respect to copper pitting.

Potentiokinetic polarization curves thus allowed the results obtained by the statistical analysis to be checked when the pitting potential was taken into account. The passivity current decreased with increase in concentration of BTAH. In contrast, for ATA and BTAOH, the passivity currents did not change with change in inhibitor concentration and the currents were always higher than those measured for BTAH. Moreover, BTAH also modified the cathodic currents which was not observed for BTAOH and ATA. This showed that BTAH was the most effective inhibitor of generalized corrosion of copper whatever the concentration.

Thus, it was very difficult to compare the efficiency of the three inhibitors towards pitting corrosion and towards generalized corrosion. To better understand these results, electrochemical impedance measurements were performed. This technique was completed by XPS analysis.

### 3.4. Impedance measurements

Impedance measurements on the copper electrode in solution, with and without the inhibitors, were performed after one hour of polarization at an anodic potential of +400 mV vs SCE. Various concentrations of inhibitors were tested. Figure 5 presents the impedance diagram, plotted in Bode coordinates, obtained without inhibitor. The diagram is characterized by two time constants. The first is well defined in the middle-frequency range and, in the very low frequency range, the beginning of a second time constant is observed. The diagram accounts for the presence of a passive layer in agreement with a high value of the impedance modulus. Thus, the low-frequency part of the diagram can be attributed to a diffusional process in the solid phase [7, 23] which controls the growth of the passive layer.

Figure 6 represents the impedance spectra obtained in the presence of BTAOH. Whatever the BTAOH concentration, the diagrams are superimposable. In addition, the spectra have a similar shape to that obtained without inhibitor under the same experimental conditions. Quantitatively, small increases in the maximum of the phase and the modulus can be observed. Compared to the system without inhibitor, these observations indicate that the effect of BTAOH on the passive layer is low and independent of the concentration.

Figure 7 shows the diagrams obtained for different concentrations of ATA. These are strongly influenced by change in ATA concentration. A single time constant appears which is better defined at higher concentration. It is surprising to note that the modulus of the impedance decreases as the concentration increases (Table 1).

In the presence of BTAH (Figure 8), the modulus is very high and accounts for a significant modification of the interface linked to strong interactions between BTAH and copper oxide [11–13]. The resistivity of the film was higher than that measured with BTAOH and ATA. The increase in BTAH concentration leads to an increase in the modulus in the whole frequency range and to a modification of the shape of the phase in the low-frequency range. Chen et al. [21] have shown that the surface films on copper in sodium chloride solutions (pH 9) have different structures depending on the BTAH concentration. They gave a value of the critical concentration of BTAH of 0.17 mM. Above this critical concentration CuO disappears in the multilayered surface film resulting in an increase in the inhibitive efficiency. In our work, the experiments were carried

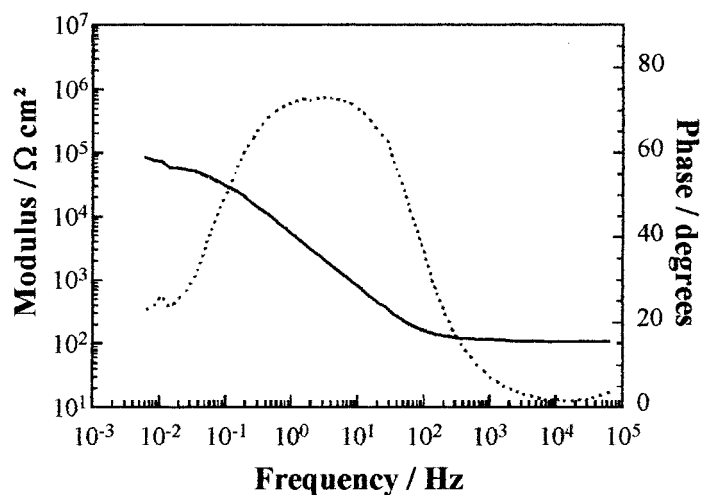


Fig. 5. Bode plots for copper polarized for 1 h at +400 mV vs SCE in borate-buffered solutions.  $\Omega = 1000$  rpm. Key: (—) modulus and (.....) phase.

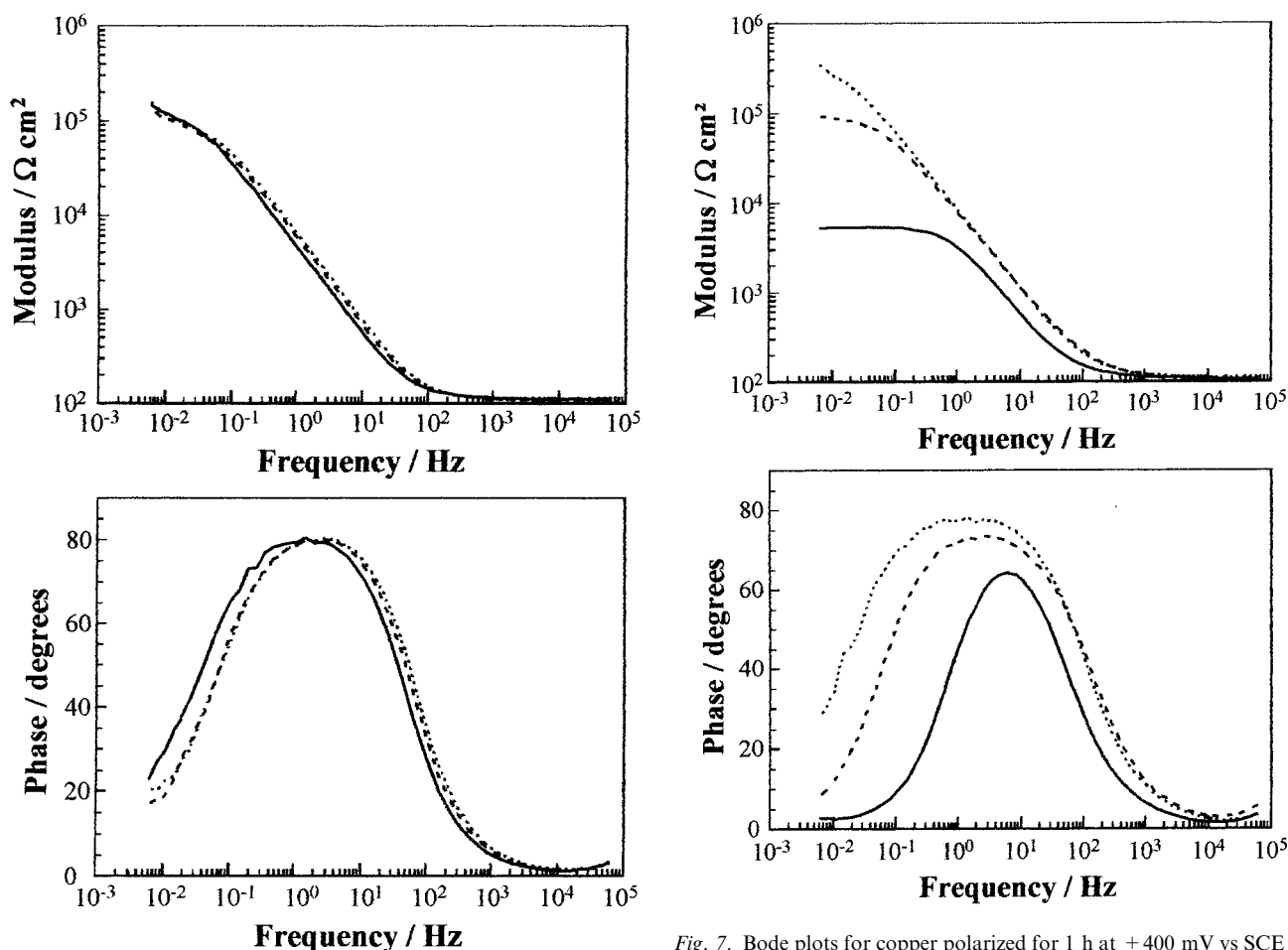


Fig. 6. Bode plots for copper polarized for 1 h at +400 mV vs SCE in borate-buffered solutions in presence of  $10^{-2}$ ,  $10^{-3}$  or  $10^{-4}$  M BTAOH.  $\Omega = 1000$  rpm. Key: (—)  $10^{-2}$  M, (---)  $10^{-3}$  M and (.....)  $10^{-4}$  M.

out from each part of this critical concentration and may explain the difference in behaviour.

Impedance measurements revealed that BTAH leads to the formation of a very protective film. The copper-solution interface was poorly modified in the presence of

Fig. 7. Bode plots for copper polarized for 1 h at +400 mV vs SCE in borate-buffered solutions in presence of  $10^{-2}$ ,  $10^{-3}$  or  $10^{-4}$  M ATA.  $\Omega = 1000$  rpm. Key: (—)  $10^{-2}$  M, (---)  $10^{-3}$  M and (.....)  $10^{-4}$  M.

BTAOH. The electrochemical behaviour of the interface was independent of the concentration of the two compounds. Conversely, for ATA, the film formed was not very protective and its resistance decreased with increasing concentration. This indicates a strong modification of the film in the presence of ATA.

Table 1. Influence of the ATA concentration on the impedance modulus for copper polarized for 1 h at +400 mV vs SCE in borate-buffered solutions

[ATA]/M	$R_p/\Omega \text{ cm}^2$
$10^{-4}$	400 000
$10^{-3}$	80 000
$10^{-2}$	5200

### 3.5. XPS analysis

XPS analysis was carried out on a copper surface treated with the different inhibitors at  $10^{-4}$  M and  $10^{-2}$  M. The copper surface treated in a borate-buffered solution was considered as reference.

At  $10^{-4}$  M, the spectra related to BTAH and BTAOH did not show the presence of nitrogen. A weak peak of nitrogen was only detected for ATA. It should be noted that XPS is not a very sensitive technique. Thus, the absence of a nitrogen peak for BTAH and BTAOH does not mean that the compounds are not present on the surface. Conversely, for ATA, the detection of nitrogen peak does indicate that this inhibitor significantly reacts with the sample surface even at low concentration.

The C, O or N to Cu atomic ratios on the surface after treatment in solution without inhibitor and in the

Table 2. Atomic ratios deduced from XPS measurements on the surface of copper polarized for 1 h at +400 mV vs SCE in borate-buffered solutions without or with  $10^{-2}$  M BTAH, BTAOH or ATA

Atomic ratio	Reference	BTAH	BTAOH	ATA
O/Cu	1.03	1.92	11.9	0.77
C/Cu	1.02	9.61	12.2	1.90
N/Cu	—	1.64	2.8	0.89

presence of BTAH, BTAOH and ATA at  $10^{-2}$  M are given in Table 2. Whatever the treatment, oxygen, carbon and copper were detected. In the presence of inhibitors nitrogen was also detected.

For BTAOH and BTAH, the atomic ratios O/Cu, C/Cu and N/Cu were high and, conversely, very low for ATA. These differences show that the film formed in the presence of ATA is different from those developed with BTAOH and BTAH. The low quantities of oxygen for ATA in comparison with those measured for the two other compounds, and even for the reference, suggest that the oxide film is thinner in the presence of ATA.

For each inhibitor and for the reference, the XPS spectra of the Cu  $2p_{3/2}$  region and the Auger spectra of the Cu LMM peak were deconvoluted (Figure 9). The Cu  $2p_{3/2}$  peak is in fact composed of two peaks. The peak at 932.4 eV is related to  $\text{Cu}_2\text{O}$  and to metallic Cu, and the other one at 934.2 eV is attributed to CuO. But, this second peak is broad for BTAH and BTAOH by comparison to the first one. This suggests the existence of a third peak which could be attributed to a link between copper and the organic molecules. For ATA, the second peak also seemed to be broad; however, it is too weak to be accurately defined. The quantitative analysis of the XPS spectra of the Cu  $2p_{3/2}$  region shows that for BTAH and ATA the proportion of CuO was much lower than that for reference and BTAOH.

The deconvolution of Auger spectra of the Cu LMM peak confirmed these results. The spectra obtained for the reference was, in fact, composed of three peaks: Cu (918.7 eV), CuO (918.0 eV) and  $\text{Cu}_2\text{O}$  (917.0 eV). Comparison with the spectra obtained for the three inhibitors shows that for BTAH and BTAOH, a fourth peak appeared close to 914 eV. This peak can be related to the existence of a link between Cu and the organic molecule. For ATA, only three peaks were observed because that related to CuO completely disappeared indicating a thinner passive film. For this inhibitor a link between copper and the organic compound also appeared (peak at 914.4 eV).

The results showed that the film formed in the presence of ATA was similar to that formed with BTAH. However, XPS measurements showed that the ATA molecule adsorption on the surface of copper prevented the formation of the CuO layer and thus the passive film was thinner. This was corroborated by the smaller impedance modulus with increasing ATA concentration.

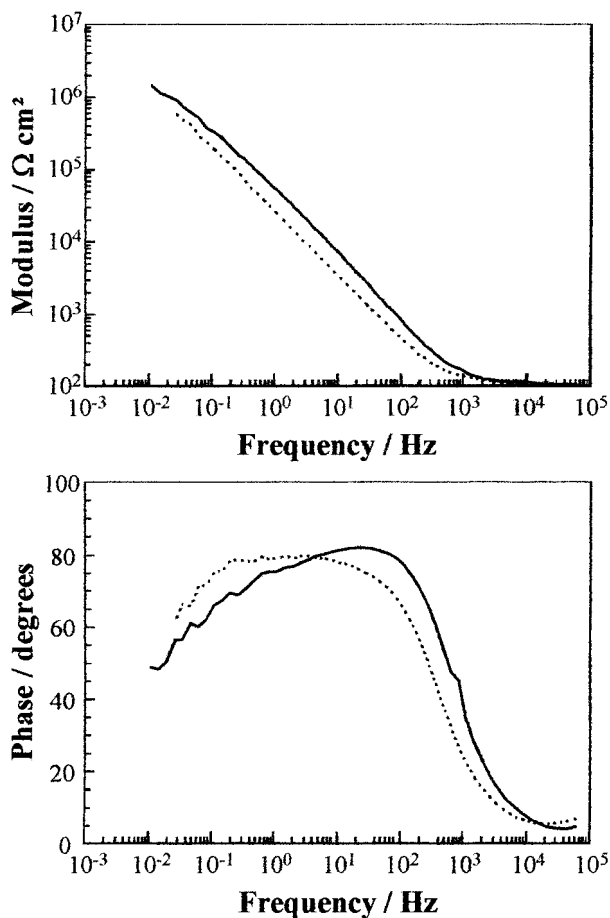


Fig. 8. Bode plots for copper polarized for 1 h at +400 mV vs SCE in borate-buffered solutions in presence of  $10^{-4}$  or  $10^{-2}$  M BTAH.  $\Omega = 1000$  rpm. Key: (—)  $10^{-2}$  M and (.....)  $10^{-4}$  M.

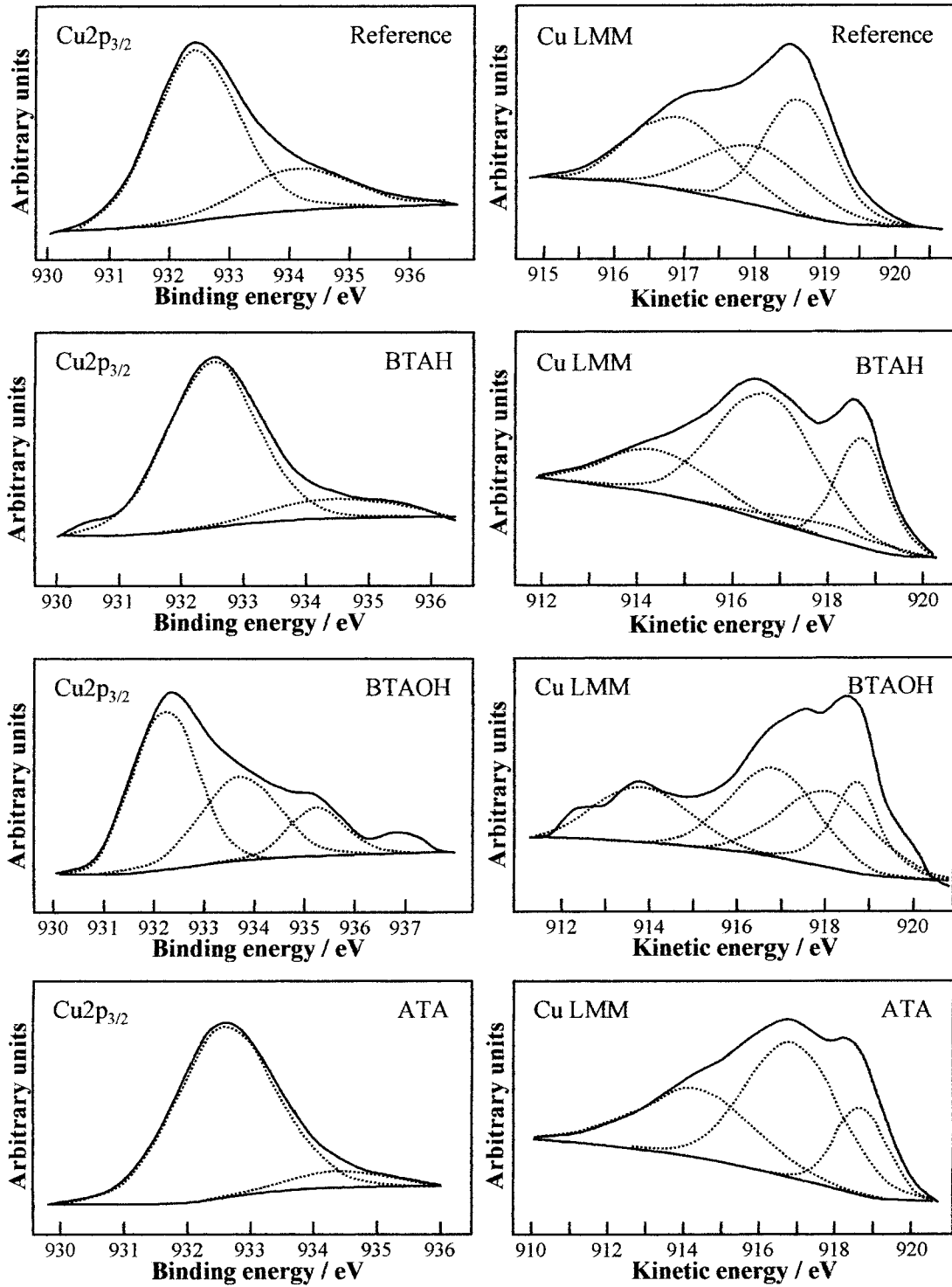


Fig. 9. XPS spectra of the Cu  $2p_{3/2}$  region and Auger spectra of the Cu LMM peak for copper polarized for 1 h at +400 mV vs SCE in borate-buffered solutions with or without  $10^{-2}$  M BTAH, BTAOH or ATA.

#### 4. Conclusions

ATA was the most efficient inhibitor towards copper pitting even though it made the passive film thinner. However, BTAH remains the better inhibitor for protection against uniform corrosion. Thus, when localized corrosion of a material is studied, the results are often explained with reference to the properties of the passive film. This approach may be interesting when

no inhibitors are present in the solution. However, when the behaviour of a material is studied in the presence of an inhibitor, the interactions between the chloride ions and the inhibitor molecules must be considered. The role of these interactions is very significant and may explain why BTAH and BTAOH showed impedance diagrams independent of concentration but acted as inhibitors towards pitting corrosion only at high concentrations.

## References

1. W. Qafsaoui, G. Mankowski, P. Leterrible and F. Dabosi, Proceedings of the International Congress on 'Control of Copper and Copper Alloys Oxidation', Rouen, France (1992) and *Revue de Métallurgie*, série 6 (1992), p. 63.
2. P.E. Francis, W.K. Cheung and R.C. Pemberton, Proc. 11th Int. Corr. Cong., Florence, Italy, Ed. Associazione Italiana di Metallurgia, Vol. 5 (1990), p. 363.
3. J.P. Duthil, G. Mankowski and A. Giusti, *Corros. Sci.* **38** (1996) 1839.
4. T. Shibata and T. Takeyama, *Corrosion* **33** (1977) 243.
5. W. Qafsaoui, G. Mankowski and F. Dabosi, *Corros. Sci.* **34** (1993) 17.
6. R. Walker, *Corrosion* **29** (1973) 290.
7. R. Babic, M. Meticos-Huković and M. Loncar, *Electrochim. Acta* **44** (1999) 2413.
8. S. Ferina, M. Loncar and M. Meticos-Huković, Proceedings of the 8th Symposium on 'Corrosion Inhibitors', Ferrara, Italy (1995), p. 1065.
9. F. Chaouket, A. Srhiri, A. Ben Bachir and A. Frignani, Proceedings *op. cit.* [8], p. 1031.
10. C. Fiaud, Proceedings *op. cit.* [8], p. 929.
11. J.B. Cotton and I.R. Scholes, *Br. Corr. J.* **2** (1967) 1.
12. G.W. Poling, *Corros. Sci.* **10** (1970) 359.
13. F. El-Taib Heakal and S. Haruyama, *Corros. Sci.* **20** (1980) 887.
14. D. Tromans, *J. Electrochem. Soc.* **145** (1998) L42.
15. P.G. Fox, G. Lewis and P.J. Boden, *Corros. Sci.* **19** (1979) 457.
16. R. Youda, H. Nishihara and K. Aramaki, *Electrochim. Acta* **35** (1990) 1011.
17. G. Xue, J. Ding, P. Lu and J. Dong, *J. Phys. Chem.* **95** (1991) 7380.
18. D. Chadwick and T. Hashemi, *Corros. Sci.* **18** (1978) 39.
19. C. Tornkvist, D. Thiery, J. Bergman, B. Liedberg and C. Leygraf, *J. Electrochem. Soc.* **136** (1989) 58.
20. I.C.G. Ogle and G.W. Poling, *Can. Met. Quartely* **14** (1975) 37.
21. Chen Jin-Hua, Lin Zhi-Cheng, Chen Shu, Nie Li-Hua and Yao Shou-Zhuo, *Electrochim. Acta* **43** (1998) 265.
22. A. Laachach, M. Aouial, A. Srhiri and A. Ben Bachir, *J. Chim. Phys.* **89** (1992) 2011.
23. Y. Feng, W.K. Teo, K.S. Siow, K.L. Tan and A.K. Hsieh, *Corros. Sci.* **38** (1996) 369.